

Linear viscoelastic properties of extruded amorphous potato starch as a function of temperature and moisture content

Magdalena Kristiawan¹ · Laurent Chaunier¹ · Guy Della Valle¹ · Denis Lourdin¹ · Sofiane Guessasma¹

Received: 9 October 2015 / Revised: 5 March 2016 / Accepted: 20 April 2016 / Published online: 28 April 2016
© Springer-Verlag Berlin Heidelberg 2016

Abstract The effects of temperature and moisture content on the linear viscoelastic behavior of extruded amorphous potato starch were studied using dynamic mechanical analysis (DMA) from the glassy to the rubbery state. Sinusoidal tensile tests were carried out in multifrequency mode in the range of 0.1–40 Hz, with a temperature ramp of 20 to 135 °C. The water loss during DMA thermal scanning was evaluated by gravimetric analysis of batch sampling in parallel experiments that simulated temperature evolution. Loss and storage moduli were then corrected on real moisture content. Using the time–temperature superposition principle, master curves were obtained for loss and storage moduli over 18 decades in frequency. The generalized Maxwell model, in the form of a Prony series obtained from master curve fitting, was used to predict the relaxation modulus. Results showed that the relaxation modulus varied over a wide range, from 2650 MPa ($t=10^{-2}$ s, 20 °C, 8 % w.b.) to 0.16 MPa ($t=10^5$ s, 95 °C, 16 % w.b.). The obtained constitutive equation was effective to predict the linear viscoelasticity behavior of potato starch in a wide range of thermomechanical conditions, as shown by the results of simulations of tensile experiments using finite elements.

Keywords Extrusion · Dynamic thermo-mechanical analysis · Time–temperature superposition · Linear viscoelasticity · Generalized Maxwell model · Water loss

Introduction

The use of starch-based materials is limited in engineering applications because of their sensitivity to water and aging. Starch consists of two main polysaccharides, linear amylose and highly branched amylopectin, both based on chains of α -(1 → 4)-linked D-glucose monomers. In its native form, starch is stored in plants in the form of granules and presents a semicrystalline structure. Beyond the melting temperature, the value of which depends on starch moisture content (*MC*), the crystallinity disappears and the starch becomes amorphous (Donovan 1979).

The variation of the water content also shifts the glass transition temperature T_g . When the material is stored at a temperature $T > T_g$, recrystallization of amylose and amylopectin is expected due to molecular reorganization (Bizot et al. 1997; de Graaf et al. 2003; Van Soest and Knooren 1997). The glass transition governs the processing of materials, especially shaping. It also affects any physical behavior that depends on molecular mobility, including mechanical properties (Chung and Lim 2006; Van Soest et al. 1996; Van Soest and Knooren 1997). The effects of moisture and various plasticizers on the mechanical properties of extruded starch were studied by Shogren (1993) and Stading et al. (2001), who demonstrated the plasticization of the amorphous phase by water.

Véchambre et al. (2009) demonstrated the shape memory property of the extruded starch. The starch recovered its initial (permanent) shape after being deformed into a temporary shape. The shape recovery can be triggered by *pH* change, moisture uptake that lowers T_g , and heating above T_g . This functional property increases the field of application of amorphous starch and emphasizes the need for better knowledge of the rheological properties of starch, including viscoelasticity in the domain of glass transition.

✉ Magdalena Kristiawan
magdalena.kristiawan@nantes.inra.fr

¹ INRA, UR 1268 Biopolymers Interactions and Assemblies (BIA), BP 71627, 44316 Nantes, France

Viscoelasticity refers to the distinctive ability of materials to exhibit both viscous and elastic properties (Ferry 1980). A linear viscoelastic material is a material that has a linear relationship between its strain history and its current value of stress. In this case, the material is submitted to deformation or stress small enough so that its rheological functions do not depend on the value of deformation or stress.

Until now, the linear viscoelastic behavior of starchy films in relation to glass transition was studied by dynamic mechanical analysis (DMA) at a single frequency and moisture content (Chanvrier et al. 2005; Chaunier et al. 2012; Shogren 1992). The DMA test is more accurate and convenient than the stress relaxation test (uniaxial quasi-static test) to investigate the material response to short time loading under low strain. On the other hand, the stress relaxation experiments can be used for the study of large deformations, i.e., for non-linear viscoelasticity, keeping in mind that to account for real processing situations, the linear viscoelasticity model, which is valid for small deformations, must be extended to describe large deformations. In the past, frequency sweeps were only rarely applied to highlight the structural differences between rubbery and glassy extruded starches (Della Valle et al. 1998).

The knowledge of the mechanical properties of starch materials around the glass transition is still incomplete, and there is no general constitutive equation for the mechanical behavior of starch when crossing T_g . Furthermore, none of the authors that studied the effect of moisture content on starch viscoelasticity has taken dehydration during analysis into consideration.

The aim of this study was to measure the linear viscoelastic properties of amorphous potato starch by DMA and to determine a constitutive law as a function of temperature and moisture content involving the glass transition that can be further used for simulation purposes. This study was initiated by our original experimental results about tensile tests on extruded starch with different moisture contents and temperatures, which are presented first here. For this purpose, we performed DMA measurements over a wide range of experimental conditions. We took the water loss during the analysis into account, allowing corrections of E' and E'' data on the real moisture content. The water loss was measured by batch sampling during an experiment that simulated temperature–time dependence during DMA analysis. The time–temperature superposition principle was applied to extend the range of frequency (time) and to obtain master curves of $E'(\omega)$ and $E''(\omega)$. The dynamic moduli, $E'(\omega)$ and $E''(\omega)$, were described by the generalized Maxwell model using a Prony series. Thereafter, simulations were carried out using the 2D finite element method (FEM) to compare the computed results with those from the linear part of the large strain tests.

Materials and methods

Extrusion

Native potato starch was purchased from Roquette Frères (F62-Lestrem). It was stored at 4 °C and had a moisture content of 18.7 % w.b. (wet basis). The amylose/amylopectin ratio was 23/77.

Prior to extrusion, starch was mixed with water to obtain a moisture content of 26 % w.b. The mixture was then kept in a sealed glass container for 48 h at 4 °C in order to obtain a uniform humidity. Using differential scanning calorimetry (DSC) (3 °C/min) (Donovan 1979), the melting temperature corresponding to the endothermic peak of native starch with a moisture content of 26 % w.b. was found to be 104 °C with an onset at 95 °C and an offset at 117 °C.

Starch destructurezation, i.e., loss of native granular semi-crystalline structure, and blending with a plasticizer, were carried out in a Scamex single-screw extruder (Rheoscam Type 20.11d, Crosne, France) using a flat die (section $30 \times 0.8 \text{ mm}^2$; length: 39 mm). The total length of the barrel and screw was 200 mm, the ratio of the screw length and diameter (L/D) was 10, and the screw speed was 15 rpm. The temperature profile along the barrel from the feed to the exit zone was characterized by temperatures of 100, 115, 110 and 105 °C. This temperature profile was set to obtain the melting of the starch granules in the first part of the extruder and to prevent expansion of the starch melt at the die exit.

Under these conditions, the material temperature at the die exit was 118 °C; the pressure at the die inlet, 17 MPa; the torque, 15 N.m; and the feed rate, 3.5 g/min, which led to a specific mechanical energy of approximately 400 J/g. The extruded ribbons did not exhibit any significant expansion. They were cut into 20–30-cm long pieces, which were stamp-cut into rectangular parallelepiped specimens measuring $25 \times 5 \text{ mm}^2$ and into dog-bone specimens with a dimension consistent with ISO 527-2-5A (Brown 2002). All of the specimens were then equilibrated in a controlled humidity environment. Since the ribbon thickness slightly varied ($\pm 5 \%$) around a nominal value of 1.1 mm, the specimen dimensions were corrected for differences in the thickness.

Analytical methods

Specimen conditioning and moisture content

All specimens were air-dried at ambient temperature for 3 days and then conditioned at relative humidity $RH = 59 \%$ and 20 °C for 1 week. After this initial storage period, the moisture conditioning of the specimens was achieved by storage at 20 °C for 4 weeks in sealed desiccators at a controlled humidity of $20 \leq RH \leq 79 \%$ over saturated salts, to obtain the moisture contents 9.3, 10.6, 12.4, 14.2, 15.5, 16.3, and 17.2 % wet

basis (w.b.). Mold growth at high relative humidities ($RH > 0.75$) was avoided by placing a test tube containing the biocide, sodium azide (NaN_3), in the desiccator (Pacheco-Palencia et al. 2007). The presence and evolution of crystallization during storage were checked every week by X-ray diffraction (wide angle x-ray scattering analysis (WAXS)), as described below.

The moisture contents of the native starch powder and equilibrated specimens were determined gravimetrically in a Chopin oven at 130 °C for 72 h. They were also deduced from T_g measurements using DSC.

Glass transition temperature

The glass transition temperature T_g was determined by differential scanning calorimetry (DSC) using a T.A. Q100 instrument (TA Instruments, New Castle, DE, USA). The system was calibrated with indium. Measurements were carried out with 10 mg samples sealed in aluminum cells to prevent water loss during analysis. Two successive scans were run at 3 °C/min between 10 and 120 °C (or 150 °C for a moisture content of less than 11 % w.b.), separated by a cooling stage, to eliminate any thermal event due to aging during storage. The glass transition temperature was determined at the midpoint of the calorific capacity change during the second scan.

The temperature of the main mechanical relaxation (T_α) related to the calorimetric glass transition temperature (T_g) was evaluated from the maximum peak of the loss modulus at 1 Hz. In this study, T_α is also denoted as mechanical T_g . If the mechanical attribute is not used, all the T_g mentioned should be considered as calorimetric T_g .

Structural changes in starch

The degree of starch transformation was determined using the decrease of the DSC residual gelatinization enthalpies of extruded starch after 4 weeks of equilibration at $RH = 59$ % and 20 °C. Approximately 40 mg of deionized water was added to 10 mg of cryoground samples in the sealed stainless steel cells. The second cell containing 50 mg of water was used as a reference. The DSC scans were run at 3 °C/min from 10 to 120 °C. No significant value for residual gelatinization enthalpy was detected, meaning that the material was amorphous directly after processing.

WAXS was used to determine the crystallinity index of conditioned specimens according to the method described by Bello-Pérez et al. (2005). The analysis was performed using a Bruker D8 (Bruker AXS Inc., Fitchburg, WI, USA) diffractometer equipped with a copper source and operating at 40 kV and 40 mA.

Tensile test

The quasi-static mechanical tests were carried out on a Synergie 100 (MTS, Eden Prairie, MN, USA) equipped with a 100-N load cell. In order to control the temperature, the tensile apparatus was equipped with a device specifically designed in the laboratory that made it possible to immerse the specimen in a silicon oil bath at a selected temperature. The tests were performed on dog-bone specimens with selected moisture contents at fixed temperatures, from the glassy to the rubbery state. The crosshead speed was set at 20 mm/min, which corresponded to the strain rate value of 0.0167 s^{-1} . The specimen gauge length was 20 mm. All experiments were repeated three times. At the beginning, the specimen was fixed between the clamps and preheated in the silicon oil bath for 30 s in order to obtain thermal equilibrium. The engineering stress data were converted to true stress assuming a Poisson's ratio of 0.38 (Zhou et al. 2009). All tensile measurements were replicated and the reported values are the averages of at least three measurements. The relative error was less than 10 %.

Dynamic mechanical analysis

A DMA apparatus (Metravib DMA50, France) was used in the tensile mode with constant strain amplitude of 0.05 %. This value was in the range of the linear viscoelasticity of amorphous starch (Della Valle et al. 1998; Ditudompo et al. 2013). DMA was applied on bar specimens in the combined sweep mode: multiple frequencies of 0.1, 0.3, 1, 3, 10, and 40 Hz and a temperature sweep from 20 to 135 °C. The heating rate was set at 3 °C/min. The temperature measured by a thermocouple placed close to the sample differed by less than ± 0.3 °C compared to the sample bulk temperature. The measurements at the different frequencies were taken at different periods of time. Therefore, the values of E' , E'' , and corresponding sample temperatures were not recorded at constant time intervals. At least 27 values of complex dynamic moduli were recorded for each frequency in the given temperature range.

The distance between apparatus grips was 20 mm and the specimen extremities were fixed at a length of 2.5 mm.

Prior to DMA, the specimen surface was coated with a thin layer of silicone-based hydrophobic grease to limit dehydration during experiments. It has already been shown that a thin coating of grease has no effect on the thermomechanical properties of extruded starch specimens (Véchambre et al. 2011).

Nevertheless, evaporation still occurred during DMA. The variation of the moisture content during DMA was estimated in the following way. Samples were heated at the same rate and conditions as during DMA analysis. When a selected temperature was reached, the sample was removed from the DMA apparatus and the moisture content of the sample was

analyzed gravimetrically. A new sample was then heated to a higher temperature and analyzed. Six moisture contents were obtained for temperatures in the interval corresponding to the DMA analysis for every initial moisture contents. Water loss was also determined from the glass transition temperature T_g measured by DSC.

All DMA measurements were replicated and the reported values are the averages of at least three measurements. The relative error of measurement of the modulus E' and E'' was less than 8 %.

Modeling of linear viscoelasticity

Generalized Maxwell model

The viscoelastic behavior of polymeric materials can be described as a decreasing function of time: the relaxation modulus. Young's relaxation modulus $E(t)$ is defined as the ratio of time (t)-dependent tensile stress (σ_T) in the material to the applied constant tensile strain (ε):

$$E(t) = \frac{\sigma_T(t)}{\varepsilon} \quad (1)$$

The Boltzmann superposition principle, which is valid for linear viscoelastic behavior, states that the stress history can be reconstructed by adding the individual bits of strain history. For small deformations, the stress response is expressed by the convolution integral (Matsuoka 1992):

$$\sigma_T(t) = \int_{-\infty}^t E(t-\tau) \frac{d\varepsilon}{d\tau} d\tau \quad (2)$$

where t and τ are the present and past time, respectively.

This integral expresses the fading memory of the viscoelastic material. It remembers the past deformation history less than the more recent one.

The applied strain in the DMA is a periodic function of time:

$$\varepsilon(\omega) = \varepsilon_0 \sin \omega t \quad (3)$$

where ε_0 is the small strain amplitude and ω the angular frequency. The ratio of the stress over strain is defined as the complex modulus $E^*(\omega)$. This modulus can be obtained by the Laplace–Carson transformation of the relaxation modulus:

$$E^*(\omega) = j\omega \int_0^{\infty} E(t) e^{-j\omega t} dt \quad (4)$$

Linear viscoelastic behavior of polymers can be described by the generalized Maxwell model. The mechanical analogy of this model consists of a spring and N Maxwell elements (a spring and a dashpot in series) connected in parallel (Park and

Schapery 1999). Springs represent ideal solid and account for the elastic behavior, whereas dashpots stand for ideal fluid and describe viscous behavior. If the system is subjected to a constant strain, then the total stress is the sum of the stress of each element. The relaxation modulus $E(t)$ of the generalized Maxwell model is an exponentially decaying function of time represented by a discrete set of exponential decays:

$$E(t) = E_e + \sum_{i=1}^N E_i \exp(-t/\tau_i) \quad (5)$$

where E_e is the final modulus (fully relaxed modulus), E_i the i th modulus, and τ_i the i th relaxation times.

The complex Young's modulus is then calculated by substitution of Eq. 5 into Eq. 4. The real part of this modulus is Young's storage modulus $E'(\omega)$, which is in phase with the strain, and the imaginary part is Young's loss modulus $E''(\omega)$ shifted about $\pi/2$ with respect to the applied strain:

$$E'(\omega) = E_e + \sum_{i=1}^N E_i \frac{(\tau_i \omega)^2}{1 + (\tau_i \omega)^2} \quad (6)$$

$$E''(\omega) = \sum_{i=1}^N E_i \frac{(\tau_i \omega)}{1 + (\tau_i \omega)^2}$$

These relationships are referred to as the Prony series. The phase shift between stress and strain, $\tan \delta$, is defined as

$$\tan \delta = E''/E' \quad (7)$$

Model fitting

The raw data on $E'(f)$ and $E''(f)$ were treated in three steps. Firstly, for one initial moisture content, values of E' and E'' were calculated at a selected frequency for selected temperatures (25, 30, ... 105 °C) using cubic spline interpolation of the Scilab code (interp1). Secondly, the initial moisture content was replaced by actual moisture contents that were obtained as a function of temperature. Thirdly, E' and E'' were calculated for selected moisture contents (8, 10, 12, 14, and 16 % w.b.) and the selected temperatures. Thereafter, the isotherms $E'(f)$ and $E''(f)$ were transformed into $E'(\omega)$ and $E''(\omega)$.

Based on the principle of time–temperature superposition, the viscoelastic moduli isotherms were manually superposed on the reference isotherms for the temperature T_R of 50 °C by factors $a_T(T)$ along the axis ω to obtain master curves of $E'(\omega)$ and $E''(\omega)$ for each moisture content. The T_R value was chosen as a temperature lower than the lowest T_g (51.7 °C) at the maximal moisture content of 17.2 % w.b.

The parameters of the linear viscoelasticity, in our case, τ_i and E_i of the generalized Maxwell model, were obtained by fitting the shifted data $E'(\omega)$ and $E''(\omega)$ (Eq. 6) using the Genereg code (Roths et al. 2001). This code is based on the

method of Tikhonov regularization. It solves ill-posed problems that result in negative values of E_i when using a simple least square fitting method.

The relaxation modulus $E(t)$ (Eq. 5) was then expressed using the parameters of the Maxwell model obtained from DMA experiments (Eq. 6).

Model validation

Dynamic moduli and T_g

The model parameters were used to recalculate $E'(T)$ and $E''(T)$ values for the moisture content that varied in the same way as during DMA measurements. The predicted moduli were then compared to DMA raw results.

The T_α or mechanical T_g obtained from the predicted peak of $E''(T)$ at a frequency of 1 Hz was compared with the calorimetric T_g measured for different moisture contents.

Finite element method simulation of the tensile test

Using the ANSYS 12 commercial code, the achieved constitutive equation issued from DMA results were implemented into a finite element model to simulate tensile experiments under various temperature and straining rate conditions. In this code, the generalized Maxwell model of viscoelasticity was represented by the Prony series in the form

$$\alpha(t) = \alpha_e + \sum_{i=1}^N \alpha_i \exp(-t/\tau_i), \tag{8a}$$

where α_e and α_i are dimensionless spring and damper constants. Using Eq. (5), α_e and α_i are defined as

$$\alpha_i = \frac{E_i}{E_0}, \quad \alpha_e = \frac{E_e}{E_0}, \tag{8b}$$

where E_0 is the instantaneous modulus at the fast load limit ($t \rightarrow 0$):

$$E_0 = E_e + \sum E_i, \tag{8c}$$

The simulation of the elastic part of the tensile response assumed an isotropic material model, where the stress–strain relationship was fully determined based on the Prony series parameters: E_0 is the instantaneous Young’s modulus, and α_i and τ_i were defined by Eqs. 8a–8c. Poisson’s ratio ν was assumed independent of strain rate with a value of 0.38 (Zhou et al. 2009).

The Young’s modulus of the tensile tests was determined as the secant modulus at a strain of 2 % with the exception of 3 % for the temperature of 90 °C. These values were found as the best approximation of the initial part of the experimental

results. For model validation, secant moduli were calculated in the same way from the simulated stress–strain curves and compared to those obtained from the tensile experiments.

The triangular 2D quadratic element (Plane 183) was used for meshing the tensile specimen. This element is defined by six nodes with two degrees of freedom at each node: translations in the x (u_x) and y (u_y) directions. The elasticity problem was solved assuming plane stress. The irregular meshing comprises 1696 elements. The boundary conditions were applied as follows: (i) along one extremity of the dog-bone model ($y=0$ mm), the nodes were fixed in both the transverse and longitudinal directions, i.e., in the x- and y-directions; thus, $u_x = u_y = 0$ and (ii) the nodes at the other extremity ($y=45$ mm) were displaced only in the longitudinal direction, $u_x = 0$.

Results and discussion

Large strain tensile behavior

The main results of the tensile test are illustrated in Fig. 1. All curves display the same features marked by a sharp initial, nearly linear, increase of stress, namely the elastic part, followed by a smooth decrease ($T < T_g$) or increase ($T > T_g$), which can reflect either a plastic or a hyperelastic behavior before rupture. The amorphous starch clearly behaves more like a brittle material at $T < T_g$, with a large Young’s modulus (initial slope) and low strain values at break. Conversely, at $T > T_g$, more ductile behavior is seen, reflected by a lower modulus and large strain values at break. In both cases ($T < T_g$ or $T > T_g$), these characteristics vary as expected with temperature, according to molecular mobility mechanisms in

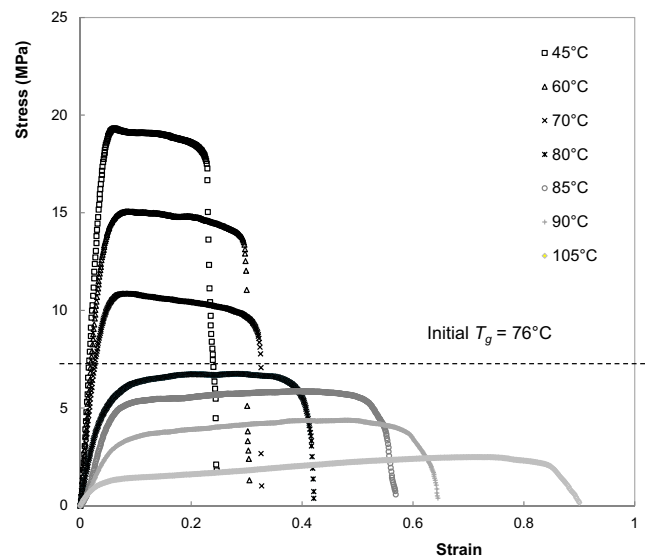


Fig. 1 Stress–strain curves obtained by uniaxial tension at a deformation rate of 0.0167 s^{-1} on amorphous potato starch ($MC = 14.2 \%$) at different temperatures

the amorphous phase. Indeed, these results are original since the behavior of amorphous starch at high temperatures and deformations has rarely been studied before. Results obtained at large strains have been more focused either on ambient temperature or high temperatures ($T \gg T_g$). In the first case, it has been shown that amylose favors larger moduli and stresses at break, probably because of its greater ability to entangle (Lourdin et al. 1995; Stading et al. 2001; Thunwall et al. 2006a). In the second case, measurements at higher temperatures ($T > 120$ °C) were performed to predict the drawability of the melt for film-blowing applications of potato starch (Thunwall et al. 2006b). In particular, the low but significant increase of stress observed here at high temperatures may be attributed to water evaporation and to starch annealing as well. Consequently, the sensitivity of extruded starch to moisture content requires a rigorous study of temperature- and moisture-dependent rheological behavior. The understanding of this behavior is important for promoting the development of starch-based biomaterials. We therefore concentrated on the study of the linear viscoelastic domain.

Raw data on the storage and loss modulus at initial moisture content

Regardless of the water content, all specimens had a crystallinity index of less than 1 %. The extruded starch was almost amorphous because there were no significant peaks at 5.6°, 10.1°, 11.3°, 14.9°, 17°, 19.5°, 22°, 23.9°, and 26° on the WAXS diagram, which are typical for B-type crystals of native/granular potato starch and retrograded starch (Van Soest et al. 1996). The slight peaks revealed with increasing moisture content only reflected the start of retrogradation and are subsequently not taken into account.

The storage and loss modulus of specimens with eight initial values of moisture content ranging from 9.3 to 17.2 % w.b. were measured at various frequencies (0.1–40 Hz) and a temperature sweep of 20–135 °C. The moduli and $\tan \delta$ are shown in Fig. 2 for the initial moisture content of 14.2 % w.b. As expected, the storage modulus decreased with increasing temperature (Fig. 2a), reflecting sample softening. The decrease of E' was rather slow until 65 °C, after which it fell rapidly until 90 °C. The latter region corresponded to the mechanical principal relaxation α associated with the glass transition. The E' curves displayed the same tendency for all frequencies. Above 105 °C, the storage modulus increased due to the water evaporation. The rubbery plateau was therefore not achieved. The storage modulus increased with the increase of the frequency, mainly beyond the glass transition. The extruded potato starch clearly displayed the behavior of amorphous polymers: as the temperature increased, it passed through the glassy region, the transition region being characterized by peaks of $\tan \delta$ and E'' and the drop in E' and, finally, through the rubbery region (Wetton 1986).

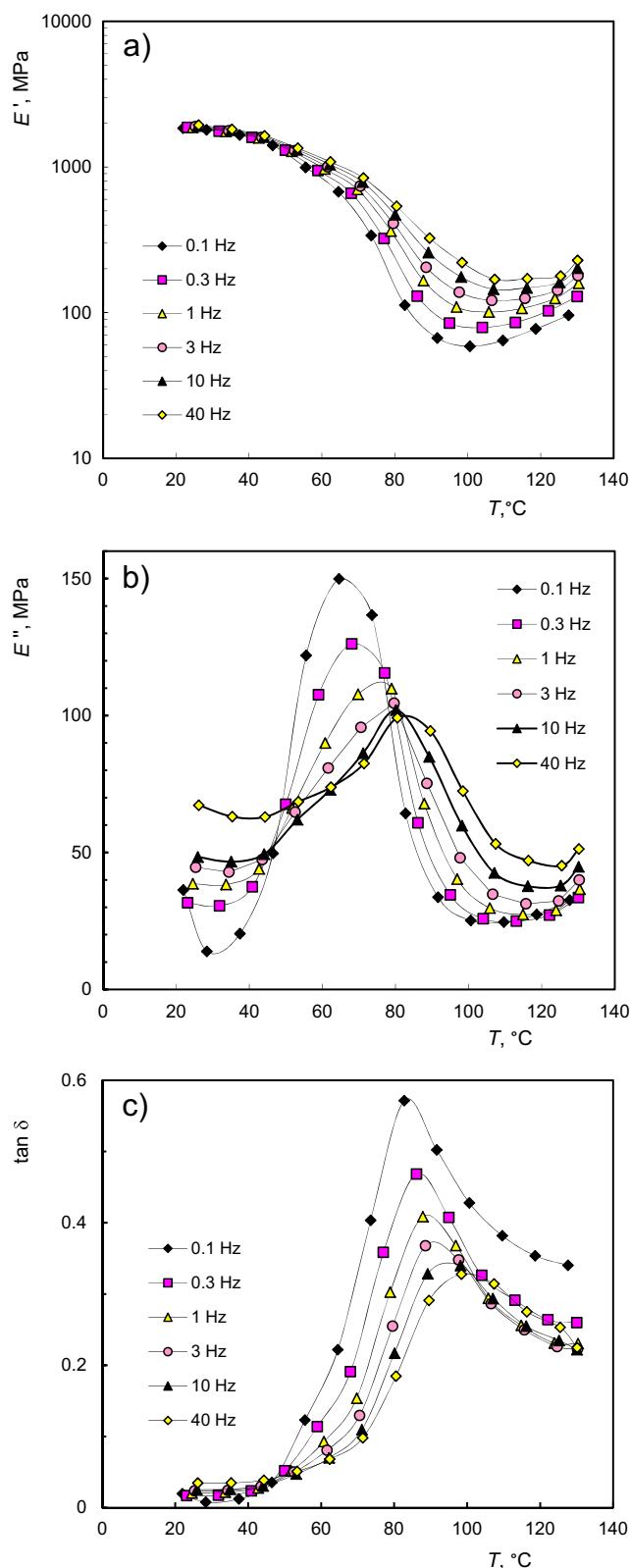


Fig. 2 Storage modulus E' (a), loss modulus E'' (b), and $\tan \delta$ (c) of extruded potato starch with an initial moisture content of 14.2 % w.b. as a function of temperature

The loss modulus exhibited a maximum for a temperature between 60 and 85 °C, depending on the frequency (Fig. 2b). This temperature increased, whereas the maximum of E'' decreased with increasing frequency. Outside this temperature interval, E'' increased with increasing frequency. All E'' curves crossed over at a temperature close to 80 °C. The phase shift $\tan \delta$ had a maximum of between 82 and 100 °C (Fig. 2c). The dependence of this maximum on frequency was the same as for E'' .

For all studied frequencies, temperatures, and moisture contents, the E' value was higher than the E'' value. This means that the phase angle between stress and strain is small and the dissipated energy is lower than the stored one. In other words, the amorphous potato starch behaved like an elastic solid, exhibiting low dissipation. The increase of E'/E'' with frequency indicated that the solid-like behavior was more pronounced with increasing frequency.

The values found here for E' , E'' , and $\tan \delta$ were in the same interval as the experimental results published in the literature and revealed the same trend as a function of temperature (Babin et al. 2007; Chaunier et al. 2012; Ditudompo et al. 2013; Shogren 1992).

The effect of dehydration during DMA is analyzed in the next section in order to correct E' and E'' based on actual moisture content.

Master curves for actual moisture content

The variation of moisture content during DMA had to be taken into account because of the significant water evaporation from the specimens, even though their surface was covered with silicon grease. The actual moisture content is shown in Fig. 3 as a function of the DMA temperature. The data were fitted by second-degree polynomials, which allowed us to attribute real actual moisture content to a sample temperature during DMA. When the sample temperature increased from 20 to 105 °C, the MC decreased from 9.3 to 8.9 % and from 15.5 to 13.8 %. The corresponding water loss was 4 and 11 %, respectively. Similar loss of moisture content was observed by Della Valle et al. (1998), whereas Ditudompo et al. (2013) reported less than 5 % and Véchambre et al. (2011) less than 3 %. These differences can be attributed to the different geometry of samples and the different modes of heating, especially to the flow of a heating medium around the sample. A decrease of about 1 % of MC was sufficient to lower the T_g by about 10 °C (Table 1), and this trend was in good agreement with the T_g dependency on MC obtained for the cast starch film reported in the literature (Lourdin et al. 1997). The rheological properties in the vicinity of the real T_g could be altered.

Using the polynomial fitting (Fig. 3), the actual moisture content was determined for every temperature. Knowing the actual moisture of each data item, the moduli $E'(f)$ and $E''(f)$ were calculated at selected moisture contents of 8, 10, 12, 14,

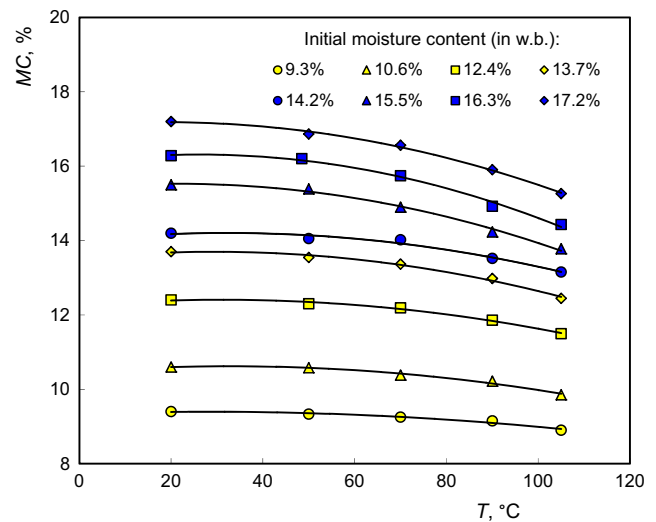


Fig. 3 Variation of moisture content during DMA analysis (heating rate 3 °C/min). The curves result from second-degree polynomial fitting ($R^2 > 0.95$)

and 16 % w.b. and temperatures in the interval of 25 to 105 °C with a step of 5 °C using interpolation and extrapolation methods. An example of $E'(f)$ and $E''(f)$ values is shown in Fig. 4 for a moisture content of 14 % w.b. with the temperature as the parameter. The storage modulus increased with an increase in frequency and decreased in temperature. Similar frequency dependencies of the moduli were observed for various types of starch-based samples. The dependence of E' on temperature for various starch origins obtained in similar conditions are compared in Table 2. The scatter of the E' values is greater for high temperatures than for low ones. This is due to different starch origins as well as to experimental errors. The values of Ditudompo et al. (2013) and Shogren (1992) seem to be too high. The small decrease of E' with increasing temperature observed by Shogren (1992) can be explained by moisture evaporation during DMA. The curve of $\tan \delta$ is not smooth, which also indicates some experimental problems. If another plasticizer is used together with water, the E' values are much lower, e.g., 0.64 MPa for wheat starch plasticized by water (MC 14 %) and glycerol (23 % w.b.) at 90 °C (Della Valle et al. 1998). They also stated that the maize starch rich in amylopectin has lower moduli compared to the starch rich in amylose. Stading et al. (2001) found that the glycerol-plasticized amylopectin film has a modulus E' (100 MPa at 20 °C and 30 MPa at 60 °C) that is ten times lower than the water-plasticized starch. The E' of amorphous potato starch

Table 1 Coefficient of Eq. 9 for $T_R = T_g$

MC	8	10	12	14	16
T_R	147	118	94.8	76.1	61.0
C_1	16.1	18.4	18.4	20.4	20.9
C_2	213	183	149	118	97.3

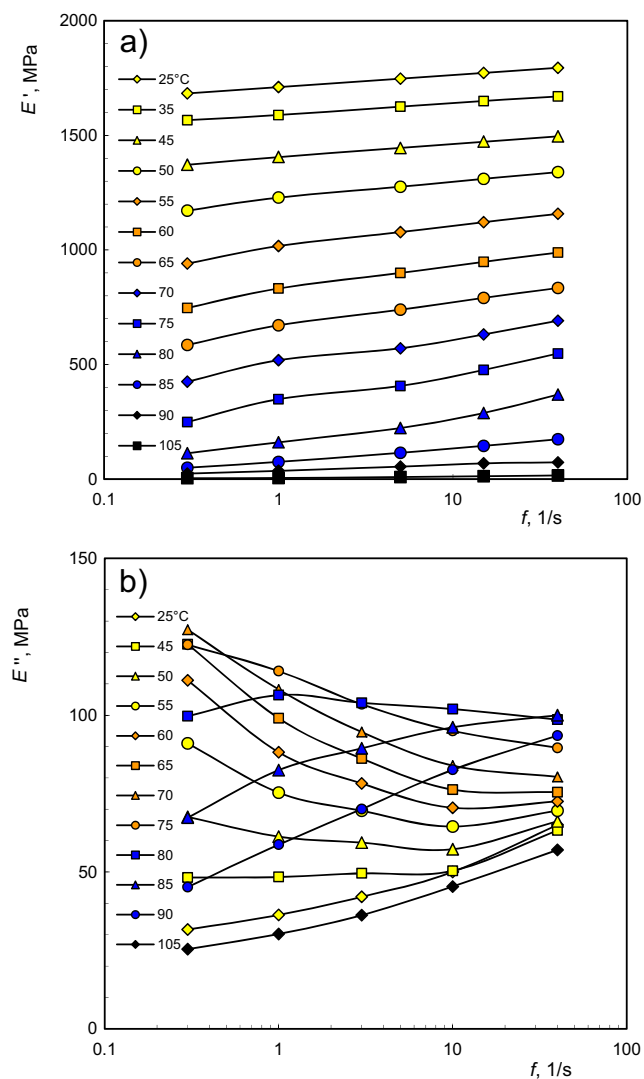


Fig. 4 E' (a) and E'' (b) moduli corrected for moisture content of 14 % as a function of frequency at different temperatures

(amylose content 23 %), in the range of 25–90 °C, was on the same order as those of amorphous maize starch obtained from the blend of high amylose maize starch and waxy maize starch, with a final amylose content of 24 % (Babin et al. 2007). As shown in Table 2, Babin et al. (2007) found that the extrudates of maize starches display decreasing E' with decreasing amylose content (or increasing amylopectin content) at the rubbery state. According to Babin et al. (2007), this trend could be attributed to the greater ability of the linear macromolecules (amylose) to entangle and thus restrict mobility compared to the highly branched ones (amylopectin) that are expected to adopt a more compact conformation. With increased frequency, more deformation energy can be stored. Conversely, with decreasing frequency, more deformation energy is lost by friction between the molecules due to increased relative motion between their chains. Hence, the material appears to be more flexible and mobile (Gottenberg and Christensen 1964). The samples therefore presented

glass-like properties when the frequency was high and the moisture content and temperature were low. Samples appeared to be more rubbery when the frequency was low and the moisture content and temperature were high.

Next, the frequency f (1/s) was converted into angular frequency ω (rad/s) in order to apply the time–temperature superposition (TTS) principle. The data on $E'(\omega)$ obtained for every selected temperature and one moisture content were superposed to fit them, in the next chapter, by a master curve at the reference temperature $T_R = 50$ °C. This was done by multiplication of ω values by factors $a_T(T)$, deduced by trial and error. The superposition consisted in shifting the E' values along the ω axis in the E' - ω diagram. The data on $E''(\omega)$ were similarly superposed using the same $a_T(T)$ factors. An example of data superposition is shown in Fig. 5a for the extruded starch with a moisture content of 14 % w.b. The same reference temperature of 50 °C was selected for all moisture contents.

The variations in shift factor with temperature were fitted by a WLF-type equation (Williams et al. 1955) and represented in Fig. 5b:

$$\log a_T = \frac{-C_1 (T - T_R)}{C_2 + (T - T_R)} \quad (9)$$

where T_R was the reference temperature of 50 °C and the constants C_1 and C_2 had values of 29.8 and 117, respectively. The standard deviation of $\log a_T$ was 0.47 ($R^2 = 0.9$). If the glass transition temperature of the amorphous potato starch was taken as the reference temperature, C_1 and C_2 were not constant. They were a function of moisture content (Table 1), which means that there is an interaction between starch and water (Williams et al. 1955).

Neither the WLF nor the Arrhenius equation (Bird et al. 1987) can account for the change of concavity of the curves representing the variations in the shift factor a_T with temperature (Fig. 5b). Therefore, a_T results were fitted by a Gompertz function:

$$\log a_T = C_1 - C_2 \exp(C_3 - \exp(-C_4 T)) \quad (10)$$

where the coefficients C_1 , C_2 , C_3 and C_4 had values of 9.60, 19.7, -6.63 , and -0.04 , respectively. The Gompertz function fitted the data better than the WLF function did with a standard deviation of $\log a_T$ 0.21 ($R^2 = 0.99$).

In the next paragraph, $E'(\omega)$ and $E''(\omega)$ are fitted by the generalized Maxwell model using Eq. 6 expressed using analytical functions.

Generalized Maxwell model

The superposed data E' and E'' were fitted by a Prony series (Eq. 6) for each moisture content. The equilibrium modulus E_e was evaluated as the asymptotic value of E' for $\omega \rightarrow 0$. Using

Table 2 Values of E' (MPa) for various extruded starches measured using DMA at different temperatures and similar conditions

Reference	Starch	MC %, f 1/s	Temperature (°C)			
			25	60	90	150
This study	Potato	14, 1	1700	830	36	
Shogren (1992)	Native maize	14, 1	4000	2150	2000	
This work	Potato	12, 1	1950	1230	630	
Chanvrier et al. (2005)	Native maize	12, 0.2	1050	900	110	
Chaunier et al. (2012)	Maize flour	12, 1	4200	3000	500	
Ditudompo et al. (2013)	Native maize	12.9, 0.1	10,640	7280	3360	
This study	Potato	9, 0.3	2100	1420	995	
Babin et al. (2007)	High amylose maize ^a	9, 0.2	3000	2100	2000	1000
Babin et al. (2007)	Maize ^b	9, 0.2	3000	2000	1500	300
Babin et al. (2007)	Maize ^c	9, 0.2	2750	1750	1100	110
Babin et al. (2007)	Waxy maize ^d	9, 0.2	2750	1100	1000	70

^a High amylose maize (starch A). Amylose: amylopectine = 70:30

^b Blend of A and B. Amylose: amylopectine = 47:53

^c Blend of A and B. Amylose: amylopectine = 23:76

^d Waxy maize (starch B). Amylose: amylopectine = 1:99

30 terms in Eq. 6, the master curves are rather smooth for both E' and E'' (Fig. 5a). Using only ten terms resulted in an acceptable curve E' , which can be used for the evaluation of the relaxation modulus, but the curve E'' exhibited large oscillations. Using 20 terms resulted in a smooth curve E' but small oscillations were still visible for the E'' curve. The standard deviations of E' and E'' were 47.0, 33.5 ($N=10$); 26.5, 6.60 ($N=20$); 26.2, 6.30 ($N=30$); and 26.0, 6.20 ($N=40$), respectively, for different numbers of Maxwell elements. The coefficient of determination R^2 of E' and E'' were 0.99, 0.97, and 0.99, respectively, and 0.21 for N equal to 30 and 10, respectively. Baumgaertel and Winter (1989) suggested that the number of relaxation modes N should be between 1 and 2 per decade of time. Therefore, in our case, for 20 decades, $N=20$ gave a good result. Subsequently, the values of E_i and τ_i for $N=20$, $MC=14\%$, and $T_R=50\text{ }^\circ\text{C}$ are given in Table 3.

The storage and loss moduli are shown in Fig. 6 for all selected moisture contents at the reference temperature of $50\text{ }^\circ\text{C}$. The storage modulus increased with decreasing moisture content. Water affected the amorphous phase, leading to the softening of the product. The loss modulus exhibited a maximum. The height and frequency of this maximum increased with increasing moisture content.

The different shapes encountered for the curves $E'(\omega)$ and $E''(\omega)$ obtained for different MC values made the application of a time–moisture superposition ineffective.

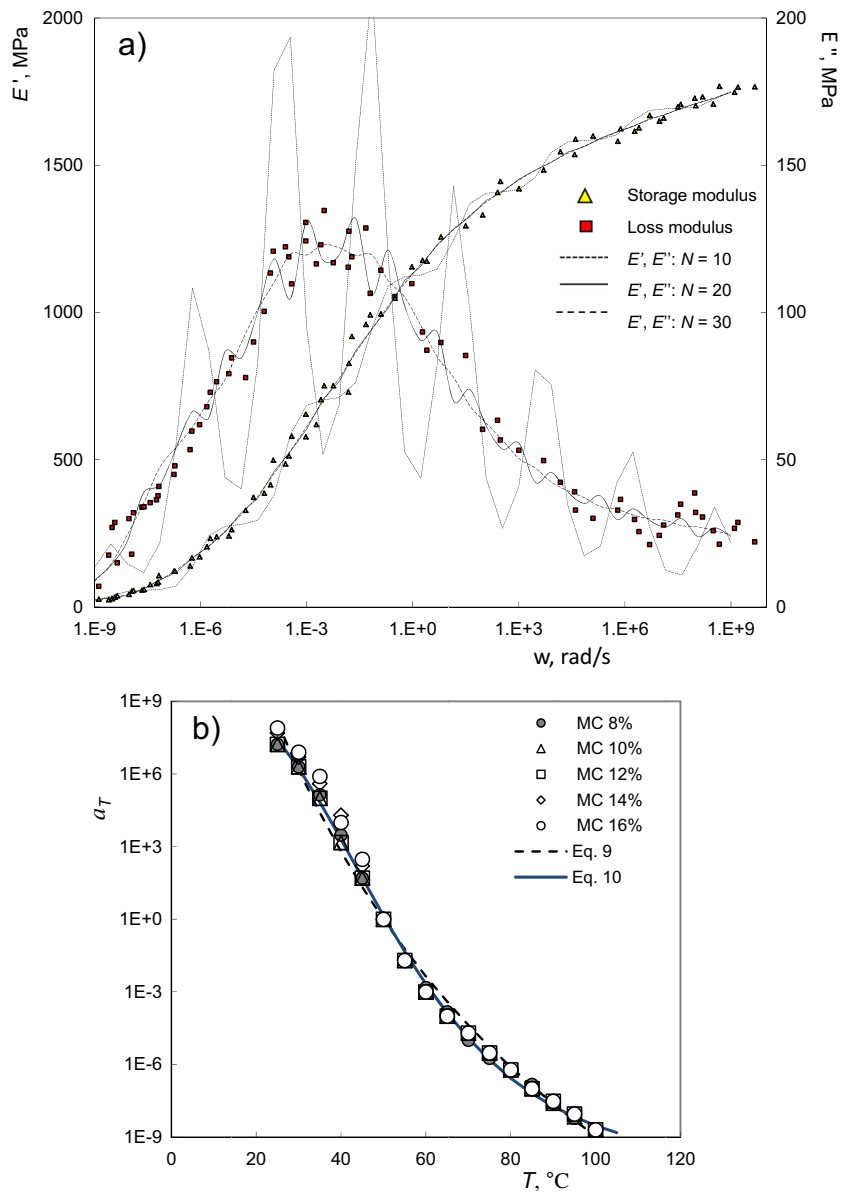
For a viscoelastic solid characterized by linear viscoelasticity, E'' should be directly proportional to ω at very low frequencies. Such behavior was not observed because the applied frequency was not sufficiently low. Since $E''(\omega \rightarrow \infty)$ was equal to zero, the function $E''(\omega)$

displayed a maximum. The temperature of this maximum can be taken as the mechanical glass transition temperature. The asymptotic value $E'(\omega \rightarrow \infty)$ was equal to the sum of E_i and E_c (elastic Young's modulus E_0).

The S-shaped curve of the storage modulus was similar to the one displayed by cross-linked amorphous solid polymers such as vulcanized Hevea rubber (Ferry 1980). The values E' and E'' of extruded potato starch were on the same order as vulcanized rubber and were much higher than those of starch plasticized with 30 % glycerol and 10 % water (Della Valle et al. 1998). This difference can be explained by a much lower content of plasticizer in our case. The storage modulus increased with increasing frequency, which indicated that the solid-like behavior was more pronounced with increasing frequency. The loss modulus exhibited a maximum at $\omega=0.003\text{ rad/s}$. Della Valle et al. (1998) found that both storage and loss moduli of wheat starch with glycerol and water increased with increasing frequency in the range of 0.06 to 60 Hz. E' was ten times higher than E'' at $\omega=0.2$, and the ratio E'/E'' increased with increasing frequency. This result indicated that elasticity prevailed over dissipation. Results obtained for isotactic polypropylene by DMA presented a similar trend over 33 decades (Keuerleber et al. 2005).

In order to have an idea about errors when the evaporation during the DMA experiment was neglected, let us consider the values of $E'=101\text{ MPa}$ and $E''=29.7\text{ MPa}$ indicated by DMA at $105\text{ }^\circ\text{C}$ and 1 Hz for the initial MC of 14.2 % w.b. (Fig. 2a, b). In fact, the actual value of MC at the time corresponding to $105\text{ }^\circ\text{C}$ was 13.1 %. By interpolating the moduli $E'(f)$

Fig. 5 Modeling of linear viscoelasticity. **a** Master curves of the measured storage (*triangles*) and loss moduli (*squares*) at 50 °C for extruded starch with a moisture content of 14 % w.b. *Solid* and *dotted* curves were calculated using *N* Maxwell elements in Eq. 6. **b** Shift factor for different moisture contents and $T_R=50$ °C. *Dotted* and *solid* curves stand for Eqs. 9 and 10, respectively



and $E''(f)$ obtained in the “Master curves for actual moisture content” section, we obtained the actual values

of E' and E'' for an MC of 14.2 % at 105 °C and 1 Hz: 40.1 and 25.4 MPa, respectively.

Table 3 Coefficients of the Prony series (Eq. 6) for extruded starch with a moisture content of 14 % w.b. at 50 °C and a relaxation time in the interval (10^{-11} , 10^{11} s) and $N=20$

<i>i</i>	0	1	2	3	4	5	6
τ_i		1.00E-11	1.44E-10	2.07E-09	2.98E-08	4.28E-07	6.16E-06
E_i	14	34.1	38.0	42.3	46.9	51.9	58.9
<i>i</i>	7	8	9	10	11	12	13
τ_i	8.86E-05	1.27E-03	1.83E-02	2.64E-01	3.79E+00	5.46E+01	7.85E+02
E_i	70.1	87.3	113	148	191	212	208
<i>i</i>	14	15	16	17	18	19	20
τ_i	1.13E+04	1.62E+05	2.34E+06	3.36E+07	4.83E+08	6.95E+09	1.00E+11
E_i	188	136	103	63.5	14.5	6.50	14.6

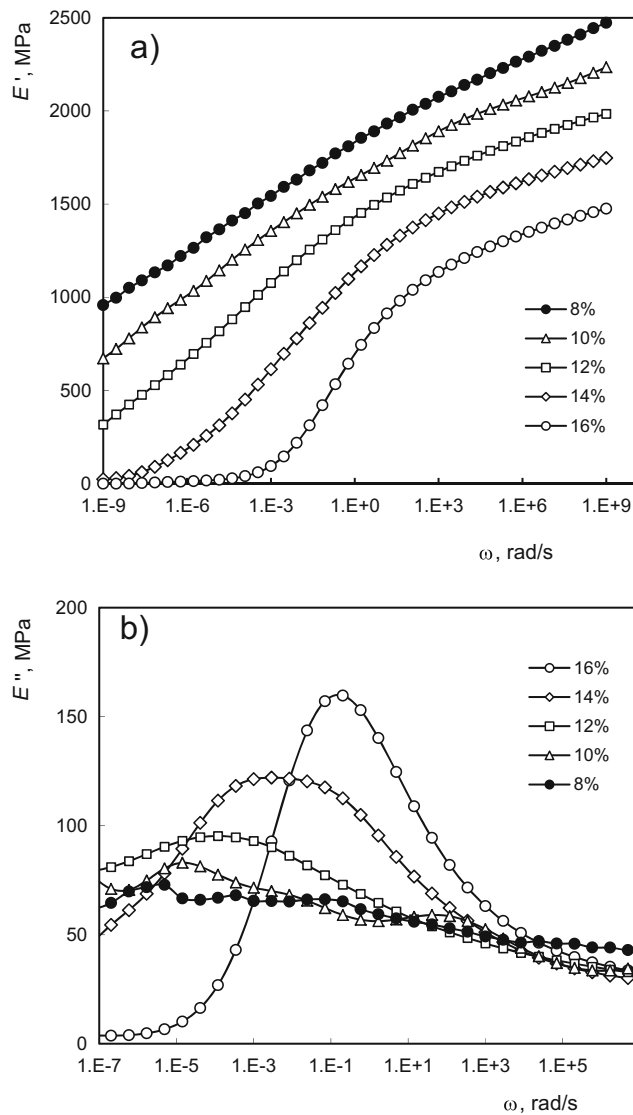


Fig. 6 Computed storage $E'(\omega)$ (a) and loss $E''(\omega)$ (b) moduli of extruded starch with different moisture contents at 50 °C. Moisture content ranges from 8 to 16 % w.b

In order to determine $E'(\omega)$ and $E''(\omega)$ for a temperature other than the reference one (50 °C), the time–temperature superposition (TTS) principle was applied. The variation of temperature was taken into account by the appropriate shift in angular frequency or time:

$$E_T'(\omega) = E_{TR}'\left(\frac{\omega}{a_T}\right), \tag{11}$$

where E_T' is the storage modulus at temperature T , E_{TR}' is the storage modulus at the reference temperature and frequency ω/a_T . For any temperature in the range of 25–105 °C, $a_T(T)$ can be computed using Eq. 10. The storage modulus was shifted toward higher ω values for temperatures lower than T_R ($a_T < 1$) and toward lower ω values for temperatures greater than T_R ($a_T > 1$).

The Relaxation Young’s modulus $E(t)$

The relaxation modulus $E(t)$ was calculated at the reference temperature using Eq. 5 with the parameters of the generalized Maxwell model ($N=20$) for the time $t=2\pi/\omega$ in the interval (10^{-9} , 10^9 s). In order to obtain a convenient expression of $E(t)$ for numerical simulations of the mechanical behavior of extruded starch, it is sufficient to determine the relaxation modulus for relaxation times in the interval (10^{-2} , 10^5 s). New coefficients E_i ($N=8$) were therefore obtained by fitting the original function $E(t)$ on the time interval (10^{-2} , 10^5 s) ($R^2 > 0.9$). The TTS principle was applied to calculate the relaxation modulus for different temperatures. It followed from the relationship $t=2\pi/\omega$ that

$$t_T = \frac{2\pi}{\omega_T} = \frac{2\pi a_T}{\omega_{TR}} = t_R a_T \tag{12}$$

The relaxation modulus was expressed as a function of temperature as $E(t_R a_T)$. The relaxation modulus was shifted toward lower time t for temperatures less than T_R and toward higher time t for temperatures greater than T_R .

The new coefficients E_i were arranged in a matrix $9(N+1) \times 16(T) \times 5(MC)$, which allows us to calculate the relaxation modulus for arbitrary variations in temperature and moisture content using an appropriate interpolation method. An example of the submatrix for $MC=14\%$ is given in Table 4. The variation of the relaxation modulus as a function of time, with temperature as the parameter, is shown in Fig. 7 for selected MC . $E(t)$ decreased with an increase in temperature and moisture content. The values of $E(t)$ varied in a wide range from 2650 MPa ($t=10^{-2}$ s, 20 °C, 8 % w.b.) in the glassy state to 0.16 MPa ($t=10^5$ s, 95 °C, 16 % w.b.) in the rubbery state. This variation was on the same order of magnitude as the variation of the Young’s modulus of amorphous waxy maize starch at room temperature from the glassy ($MC=5\%$) to the rubbery state ($MC=16\%$) (Van Soest et al. 1996).

At the same temperature, amorphous starch with lower moisture content has a longer relaxation time (higher relaxation modulus) than do a starch with higher MC (see Fig. 7). This can be explained by the greater mobility of starch chains at higher MC . The network microstructure changes from dense and homogeneous to a more open structure with fluctuations in the pore size when MC increases. The structural change is attributed to plasticization of the amorphous area by increased water content, leading to higher mobility in the network and subsequent inhomogeneous swelling (heterogeneous network) (Stading et al. 2001).

Model validation

The raw DMA results on E' and E'' obtained by varying temperature, frequency, and several values of initial moisture

Table 4 Coefficients E_i of the relaxation modulus of extruded starch with a moisture content of 14 % w.b. for the relaxation time in the interval (10^{-2} , 10^5 s)

i	e	1	2	3	4	5	6	7	8
τ_i		0.01	0.1	1	10	100	1000	10,000	100,000
E_i , 25 °C	841.0	0.9	35.9	12.6	34.1	20.8	35.6	31.0	55.9
E_i , 50 °C	125.0	11.5	100.9	62.2	123.9	90.7	118.3	90.9	86.8
E_i , 75 °C	3.8	116.2	105.8	69.7	59.4	44.6	11.6	10.6	4.5

content were simulated at a constant frequency, taking evaporation into account. The comparison between the computed and the experimental values of the different moduli is shown in Fig. 8a for an initial moisture content of 14.2 % w.b. and a frequency of 1 Hz. The predicted moduli matched the measured data with $R^2 = 0.97$ and 0.98 for E' and E'' , respectively.

The main mechanical relaxation temperature or mechanical T_g was evaluated from the peak of the predicted loss modulus

as a function of temperature at 1 Hz, and it was compared with calorimetric T_g measured using the DSC method. The predicted values of relaxation temperature were about 5 % lower than the calorimetric T_g mean values (Fig. 8b).

An ANSYS code was developed for simulation of the traction experiments. This code was a combination of the Hookean approach with the Prony series. The parameters E_0 ,

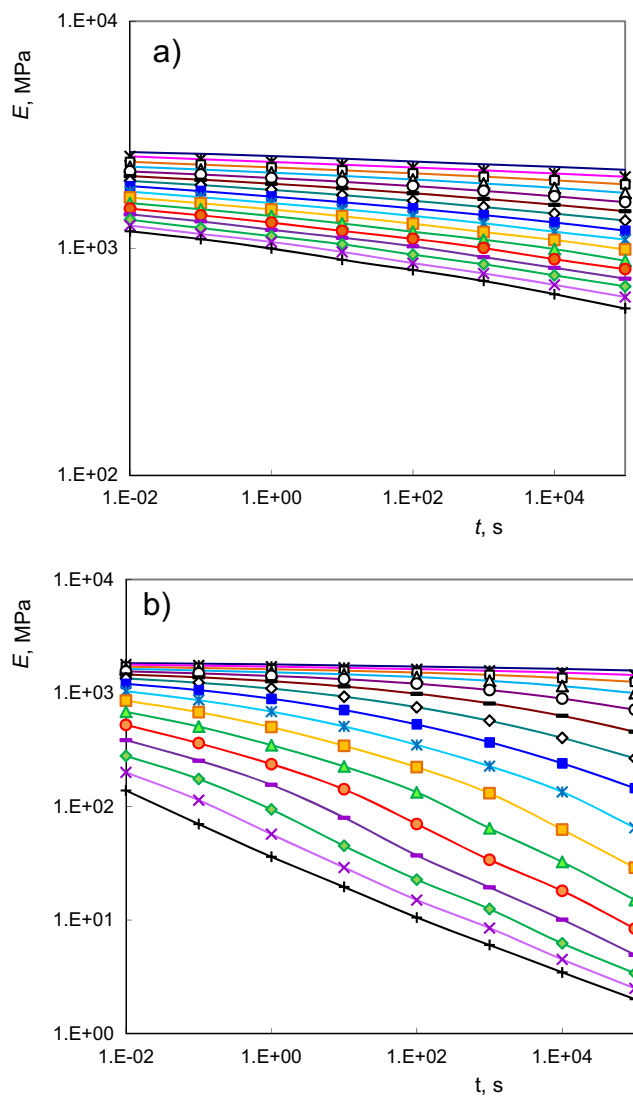


Fig. 7 Relaxation modulus as a function of time with temperature as the parameter for different moisture contents: **a** 8 %, **b** 14 % w.b. Temperature ranges from 20 °C (top curve) to 95 °C (bottom curve) with a step of 5 °C

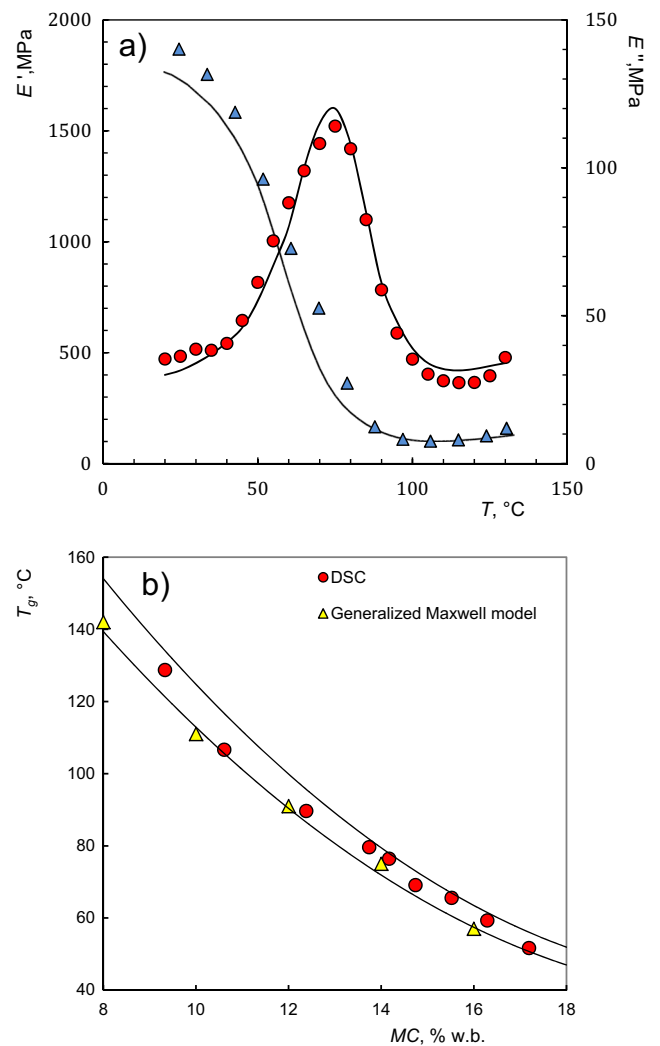


Fig. 8 Comparison between computed and experimental values for **a** storage and loss modulus at 1 Hz for an initial moisture content of 14.2 % w.b. Closed symbol—DMA data: triangles— E' , circles— E'' . Solid line—simulated data taking evaporation into account. **b** Glass transition temperature T_g measured using DSC—circles; T_g from the maxima of computed $E''(T)$ for selected moisture contents—triangles; solid lines represent ± 5 % deviation

α_i , and τ_i ($i = 1, \dots, 6$) were obtained from the relaxation modulus $E(t)$ expressed using the Prony series (Eqs. 8a–8c). The tensile simulations were carried out for different mesh sizes, but only the final fine mesh results are presented here. The subdivision of the specimen into finite elements, its deformation at a strain of 6 %, and true stress distribution in the y-direction are shown in Fig. 9 for $MC = 14.2 \%$, $T = 60 \text{ }^\circ\text{C}$, and a strain rate of 0.0167 s^{-1} . The stress is maximum and uniformly distributed along the gauge length (Fig. 9b). The specimens broke down always in this region.

The simulated stress–strain curves are compared in Fig. 10 with those obtained using traction experiments for the extruded starch with $MC = 14.2 \%$ and a strain rate of 0.0167 s^{-1} . The secant Young’s modulus computed from traction simulation is compared to the secant modulus obtained using tensile strain experiments in Fig. 11. It was difficult to obtain Young’s modulus as a tangent at the zero strain from the traction experiments, for this reason, secant moduli were determined at a strain of 2 % with the exception of 3 % for the temperature of $90 \text{ }^\circ\text{C}$. For comparison of the FEM simulations with the traction experiments, secant moduli were calculated in the same way from the simulated stress–strain curves. The error of traction experiments, estimated on 10 %, is represented by dashed lines in Fig. 11. Cumulative error of FEM results (12 %) is composed of the errors of DMA measurement, data treatment, and FEM simulation. It is represented by vertical error bars in Fig. 11.

There are some discrepancies among the results obtained from DMA, DSC, traction experiments, and numerical simulation. It is obvious that different experimental methods cannot provide exactly the same results. Starch is a biological material that exhibits some inhomogeneity resulting in property differences. With regard to these facts, we can conclude

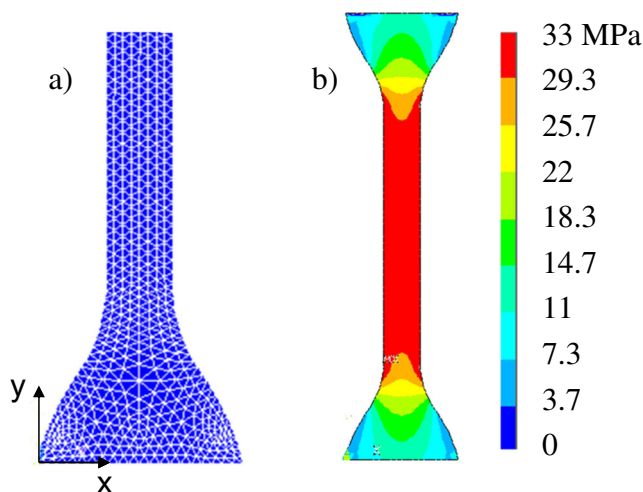


Fig. 9 FEM simulation for uniaxial traction experiment of extruded starch with $MC = 14.2 \%$ at a temperature of $60 \text{ }^\circ\text{C}$. Extensional strain = 0.06 and strain rate = 0.0167 s^{-1} . The undeformed total length is 45 mm. **a** Zoom of meshing (lower part of dog-bone). **b** Stress distribution. The stress scale is in MPa

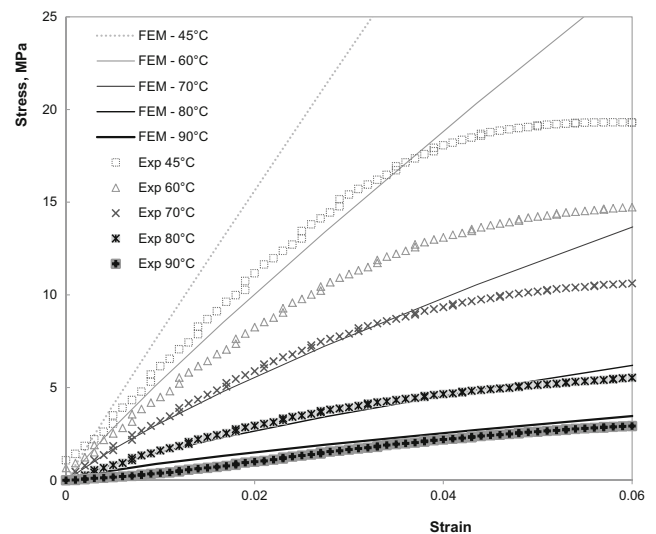


Fig. 10 Zoom of stress–strain curves measured by tensile strain experiments and simulated from DMA results using the Maxwell model of viscoelasticity represented by the Prony series. $MC = 14.2 \%$ and strain rate = 0.0167 s^{-1}

that there is an acceptable agreement among experimental data obtained by these experimental methods and simulation.

The Prony representation corresponds to the solution of the classical differential model, i.e., generalized Maxwell model of viscoelasticity. It is the key for the extension of the above constitutive equations to large deformation cases, e.g., polynomial models of strain energy potential (Neo-Hookean, Mooney-Rivlin, Ogden). Diani et al. (2012) applied a visco-hyperelasticity approach that combined a linear viscoelastic

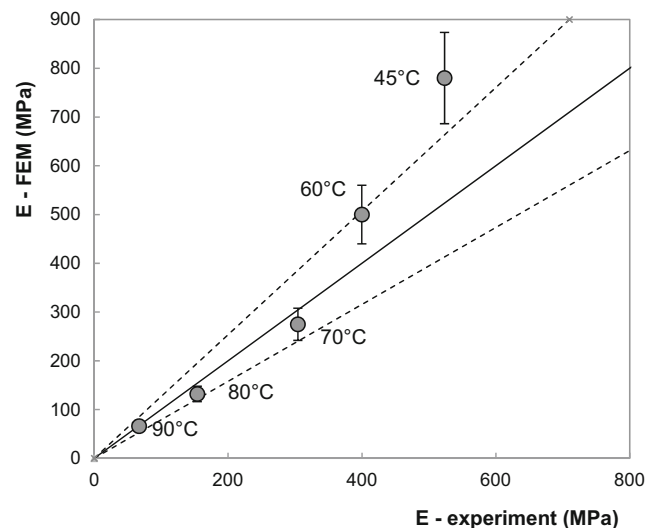


Fig. 11 Secant Young’s modulus obtained from FEM simulation using DMA results vs. tensile strain experiments. $MC = 14.2 \%$ and strain rate = 0.0167 s^{-1} . The modulus was calculated as a secant at a strain of 0.02, except for $T = 90 \text{ }^\circ\text{C}$ where a strain of 0.03 was taken into account. The dashed lines indicated an experimental error of 10 % for tensile test. The bar error on Young’s modulus indicated the cumulative error of 12 % for DMA measurement and following data treatment

model (generalized Maxwell model) with a hyperelastic model (Neo-Hookean model) to simulate shape memory effect.

Conclusions

Determining the variations of the rheological properties of extruded starch during glass transition is all the more essential for predicting its behavior during processing since it is very sensitive to moisture content. The storage and loss moduli of amorphous potato starch were therefore determined by tensile stress dynamic mechanical analysis in a wide range of frequencies as a function of temperature and moisture content. The viscoelastic moduli were corrected on the real moisture content because the moisture content of the samples decreased during DMA due to water loss. Results obtained for modulus values, mainly the storage modulus, have shown that the variation in moisture content during DMA analysis should not be overlooked.

The effect of temperature could be accounted for by using the time–temperature superposition principle, and master curves were determined. The shift factor $a_T(T)$ varied over 17 decimal orders within a range of temperature (25 to 100 °C). Its variations with temperature were fitted using a Gompertz model. No equivalent master curves for the influence of moisture content could be found.

The storage modulus E' decreased with increasing temperature and moisture content and increased with increasing frequency. The loss modulus E'' exhibited maxima as a function of MC , temperature, and frequency. In the case of a constant MC , the maximum of E'' diminished, whereas its temperature increased with increasing frequency.

The linear viscoelastic behavior of amorphous potato starch was characterized by the generalized Maxwell model using 20 Maxwell elements. In order to obtain more robust models for numerical simulations, the relaxation modulus $E(t)$ was expressed using only eight relaxation times in the interval (10^{-2} , 10^5 s), representing the domain of mechanical tests.

The main mechanical relaxation temperature values, evaluated from the maximum of computed loss modulus values, were in good agreement with the calorimetric glass transition values obtained using DSC.

The generalized Maxwell model was also validated by computing the secant modulus through finite element simulations. The agreement of this modulus with that obtained by traction experiments was in the range of experimental and computational errors, estimated on 22 %.

In light of the obtained results, the constitutive law for linear viscoelasticity of amorphous potato starch is now available for a wide range of temperature and moisture content.

Extension of the linear viscoelasticity results to large deformation cases is now possible. The Prony series obtained can be combined with a hyperelastic model. The results

presented will be used to model the shape memory property of extruded potato starch. A similar approach can be used for other starchy materials.

The proposed model could be considered as a significant contribution toward programmable rate-dependent large deformations of extruded starch under different temperatures, moisture contents and operating rates. This work will pave the way for the development of new starch-based materials (i.e., starch-based shape memory biopolymers).

Acknowledgments The authors would like to thank Bruno Pontoire of INRA BIA for the WAXS measurements.

References

- Babin P, Della Valle G, Dendievel R, Lourdin D, Salvo L (2007) X-ray tomography study of the cellular structure of extruded starches and its relations with expansion phenomenon and foam mechanical properties. *Carbohydr Polym* 68:329–340
- Baumgaertel M, Winter HH (1989) Determination of discrete relaxation and retardation time spectra from dynamic mechanical data. *Rheol Acta* 28:511–519
- Bello-Pérez LA, Ottenhof MA, Agama-Acevedo E, Farhat IA (2005) Effect of storage time on the retrogradation of banana starch extrudate. *J Agric Food Chem* 53:1081–1086
- Bird RB, Armstrong RC, Hassager O (1987) Dynamics of polymeric liquids: volume 1, 2nd edn. Wiley, New York, p 140
- Bizot H, Le Bail P, Leroux B, Davy J, Roger P, Buleon A (1997) Calorimetric evaluation of the glass transition in hydrated, linear and branched polyhydroglucose compounds. *Carbohydr Polym* 32:33–50
- Brown RP (2002) Handbook of polymer testing: short-term mechanical tests. Rapra Technology Limited, Shawbury
- Chanvrier H, Colonna P, Della Valle G, Lourdin D (2005) Structure and mechanical behaviour of corn flour and starch–zein based materials in the glassy state. *Carbohydr Polym* 59:109–119
- Chaunier L, Véchambre C, Lourdin D (2012) Starch-based foods presenting shape memory capabilities. *Food Res Int* 47:194–196
- Chung HJ, Lim ST (2006) Physical aging of amorphous starches (a review). *Starch - Stärke* 58:599–610
- De Graaf RA, Karman AP, Janssen LPBM (2003) Material properties and glass transition temperatures of different thermoplastic starches after extrusion processing. *Starch - Stärke* 55:80–86
- Della Valle G, Buleon A, Carreau PJ, Lavoie PA, Vergnes B (1998) Relationship between structure and viscoelastic behavior of plasticized starch. *J Rheol* 42:507–525
- Diani J, Gilormini P, Frédy C, Rousseau I (2012) Predicting thermal shape memory of crosslinked polymer networks from linear viscoelasticity. *Int J Solids Struct* 49:793–799
- Ditodomo S, Takhar PS, Ganjyal GM, Hanna MA (2013) The effect of temperature and moisture on the mechanical properties of extruded cornstarch. *J Texture Stud* 44:225–237
- Donovan JW (1979) Phase transitions of the starch–water system. *Biopolymers* 18:263–275
- Ferry JD (1980) Viscoelastic properties of polymers, 3rd edn. Wiley, New York
- Gottenberg WG, Christensen RM (1964) An experiment for determination of the mechanical property in shear for a linear, isotropic viscoelastic solid. *Int J Eng Sci* 2:45–57

- Keuerleber M, Woicke N, Raisch SR, Eyerer P (2005) Temperature and strain rate dependent simulation of high speed tensile tests of I-PP. *J Polym Eng* 25:411–420
- Lourdin D, Della Valle G, Colonna P (1995) Influence of amylose content on starch films and foams. *Carbohydr Polym* 27:261–270
- Lourdin D, Coignard L, Bizot H, Colonna P (1997) Influence of equilibrium relative humidity and plasticizer concentration on the water content and glass transition of starch materials. *Polymer* 38:5401–5406
- Matsuoka S (1992) *Relaxation phenomena in polymers*. Hanser Publishers, Munich
- Pacheco-Palencia LA, Hawken P, Talcott ST (2007) Juice matrix composition and ascorbic acid fortification effects on the phytochemical, antioxidant and pigment stability of açai (*Euterpe oleracea* Mart.). *Food Chem* 105:28–35
- Park SW, Schapery RA (1999) Methods of interconversion between linear viscoelastic material functions. Part I: a numerical method based on Prony series. *Int J Solids Struct* 36:1653–1675
- Roths T, Marth M, Weese J, Honerkamp J (2001) A generalized regularization method for nonlinear ill-posed problems enhanced for nonlinear regularization terms. *Comput Phys Commun* 139:279–296
- Shogren RL (1992) Effect of moisture content on the melting and subsequent physical aging of cornstarch. *Carbohydr Polym* 19:83–90
- Shogren RL (1993) Effects of moisture and various plasticizers on the mechanical properties of extruded starch. In: Ching C, Kaplan D, Thomas E (eds) *Biodegradable polymers and packaging*. Technomic Publishing Company, Inc., Pennsylvania
- Stading M, Rindlav-Westling Å, Gatenholm P (2001) Humidity-induced structural transitions in amylose and amylopectin films. *Carbohydr Polym* 45:209–217
- Thunwall M, Bolzidar A, Rigdahl M (2006a) Compression molding and tensile properties of thermoplastic potato starch materials. *Biomacromolecules* 7:981–986
- Thunwall M, Bolzidar A, Rigdahl M, Kuthanova V (2006b) On the stress-strain behavior of thermoplastic starch melts. *Int J Polym Anal Charact* 11:419–428
- Van Soest JGG, Knooren N (1997) Influence of glycerol and water content on the structure and properties of extruded starch plastic sheets during aging. *J Appl Polym Sci* 64:1411–1422
- Van Soest JGG, De Wit D, Vliegthart JFG (1996) Mechanical properties of thermoplastic waxy maize starch. *J Appl Polym Sci* 61:1927–1937
- Véchambre C, Chaunier L, Lourdin D (2009) Novel shape-memory materials based on potato starch. *Macromol Mater Eng* 295:115–122
- Véchambre C, Buléon A, Chaunier L, Gauthier C, Lourdin D (2011) Understanding the mechanisms involved in shape memory starch: macromolecular orientation, stress recovery and molecular mobility. *Macromolecules* 44:9384–9389
- Wetton RE (1986) Dynamic mechanical analysis of polymers and related systems. In: Dawkins JV (ed) *Developments in polymer characterization*. Elsevier Applied Science Publishers, London, pp 179–221
- Williams ML, Landel RF, Ferry JD (1955) The temperature dependence of relaxation mechanisms in amorphous polymers and other glass-forming liquids. *J Am Chem Soc* 77:3701–3707
- Zhou YG, Wang LJ, Li D, Yan PY, Li Y, Shi J, Chen XD, Mao ZH (2009) Effect of sucrose on dynamic mechanical characteristics of maize and potato starch films. *Carbohydr Polym* 76:239–243